Journal of Integrative Neuroscience

J. Integr. Neurosci. **2026**; 25(5): 49777
https://doi.org/10.31083/JIN49777

Original Research

The Neuroprotective Role of a Caspase-1 Inhibitor Against Apoptosis via Inhibition of Glial Hyperactivation in a Mouse Model of Epilepsy

Hui Cai[1,2,†], Xinran Xu[2,†], Xuerui Zhuo[2], Zhe Liu[1,2], Hao Liu[2], Yiming Sun[1,2,*]

[1]Pharmacy Department, The First Affiliated Hospital of Bengbu Medical University, 233000 Bengbu, Anhui, China
[2]School of Pharmacy, Bengbu Medical University, 233030 Bengbu, Anhui, China
*Correspondence: 15951977608@163.com (Yiming Sun)
[†]These authors contributed equally.

Academic Editor: Hajime Hirase
Submitted: 7 January 2026 Revised: 8 February 2026 Accepted: 24 February 2026 Published: 9 May 2026

Abstract

Background: Epilepsy is a central nervous system disorder characterized by abnormal neuronal discharges in the brain. The purpose of this study was to investigate the protective effects of a caspase-1 inhibitor on glial hyperactivation and neuronal apoptosis in epilepsy. **Methods**: A pilocarpine-induced status epilepticus (SE) mouse model was established. Belnacasan (VX765), a caspase-1 inhibitor, was administered intraperitoneally. ELISA was used to detect inflammatory cytokines interleukin (IL)-1β, IL-6, and tumor necrosis factor-alpha (TNF-α) in peripheral blood. Immunohistochemistry and transmission electron microscopy were used to evaluate glial activation and neuronal damage in the hippocampus. Western blotting was performed to detect caspase-1 and Gasdermin D N-terminal (GSDMD-N) expression. *In vitro*, primary glial cells were stimulated with lipopolysaccharide (LPS), and the effects of glial conditioned medium on HT22 neuronal apoptosis were assessed using cell counting kit-8 (CCK-8) and flow cytometry. **Results**: *In vivo* experiments showed that, as epilepsy progressed, the levels of pro-inflammatory cytokines IL-1β and IL-6 in peripheral blood were significantly increased, consistent with findings in patients with epilepsy. At 21 days after epilepsy induction, the numbers of hyperactivated microglia and astrocytes increased significantly and exhibited activation-related features such as organelle swelling, whereas neuronal numbers were markedly reduced and displayed cytological features of apoptosis. VX765 significantly alleviated seizure frequency and severity in epileptic mice and attenuated peripheral blood levels of IL-1β and IL-6, hippocampal caspase-1 activity, glial hyperactivation, and neuronal apoptosis. *In vitro* experiments demonstrated that glial conditioned medium (CMG) promoted apoptosis of HT22 neurons by regulating Bcl-2-associated X protein (Bax) and B-cell lymphoma 2 (Bcl-2) expression, whereas VX765 alleviated HT22 neuronal apoptosis by inhibiting the secretion of inflammatory factors from glial cells. **Conclusions**: These results indicate that inhibiting glial cell hyperactivation and neuroinflammation via caspase-1 inhibition may represent a potential therapeutic strategy for epilepsy.

Keywords: epilepsy; glial hyperactivation; caspase-1; VX765; neuroinflammation

1. Introduction

Epilepsy is a neurological disorder characterized by abnormal neuronal activity that affects approximately 70 million individuals worldwide [1]. The overall prevalence of epilepsy in China is approximately 1.68 per 1000 individuals [2]. Epilepsy is often accompanied by psychological, cognitive, and behavioral disorders and is associated with an increased risk of disability and accidental injury [3]. A previous study has reported that seizures are accompanied by elevated levels of inflammatory cytokines and activation of astrocytes and microglia [4]. Neuron–glial interactions are essential for maintaining synaptic homeostasis and plasticity. In addition, perivascular microglia, macrophages, and astrocytes are closely associated with cerebral microvasculature and lymphatic function [5]. However, the pathological mechanisms linking glial cell activation (astrocytes or microglia) to neuronal apoptosis during epilepsy remain poorly understood.

Glial cells account for more than 90% of cells in the brain, and their primary functions include nourishing, supporting, and protecting neurons [6]. Local or systemic inflammatory responses can lead to aberrant neural connectivity and excessive activation of glial cells. Astrocytes and microglia can transition from a resting state to an activated state in response to injury and stress, thereby maintaining brain homeostasis and limiting tissue damage [7,8]. When normal feedback mechanisms fail to resolve inflammation, glial cell–mediated inflammatory processes may promote the onset and progression of epilepsy [9]. After seizures, levels of interleukin (IL)-1β, IL-6, and other inflammatory cytokines in the brain increase significantly, possibly due to glial hyperactivation, proliferation, or pyroptosis, indicating that neuroinflammation potentially involving glial pyroptosis accompanies epileptogenesis [10]. Pyroptosis is an inflammatory form of programmed cell death triggered by caspase-1/4/5/11 and gasdermin protein activation [11,12]. However, not all caspase-1–activated cells that cleave Gasdermin D (GSDMD) and release IL-1 undergo pyroptosis. Living cells that release inflammatory cytokines through secretory pathways are considered activated or mature cells,

Copyright: © 2026 The Author(s). Published by IMR Press.
This is an open access article under the CC BY 4.0 license.

Publisher's Note: IMR Press stays neutral with regard to jurisdictional claims in published maps and institutional affiliations.

whereas dead cells releasing IL-1 are considered pyroptotic. Other cytokines exist in states different from their traditional activated or pyroptosis-induced counterparts. This unique activation state is referred to as hyperactivation [13]. This concept is consistent with the pathological manifestations observed in patients with epilepsy.

The current antiepileptic drugs are mainly Na^{+} and Ca^{2+} ion channel blockers. These drugs primarily control seizure symptoms. However, they do not prevent the development of epilepsy and are often associated with drug resistance or adverse effects [14]. Belnacasan (VX765) is an oral prodrug and a caspase-1 inhibitor capable of penetrating the blood brain barrier (BBB) [15]. This study aimed to elucidate changes in pro-inflammatory factors in peripheral blood during epilepsy progression and to investigate the effects of VX765 on microglial and astrocytic activation, glial hyperactivation, and neuronal apoptosis. In addition, the effects of glial cell–conditioned medium on neuronal injury and the protective role of VX765 against neuronal apoptosis were examined *in vitro*. Together, these findings help clarify the role of neuroinflammation regulation as a potential therapeutic strategy for epilepsy.

2. Materials and Methods

2.1 Animals and Ethics Statement

Male C57BL/6J mice (12 weeks old, weighing 25 ± 2 g) were provided by Hangzhou Zi Yuan Experimental Animal Technology [Hangzhou, Zhejiang, China]. The experimental mice were raised in a standard environment, with a room temperature of 22 ± 2 °C, humidity of 50%–60%, sufficient food and water, and a natural circadian rhythm light cycle. The experiments began one week after the animals had adapted to the environment.

The animal experiments described in this study were conducted in strict accordance with the ARRIVE guidelines and the National Institutes of Health (NIH) Guide for the Care and Use of Laboratory Animals (8th edition, 2011). All efforts were made to minimize animal suffering and reduce the number of animals used. In accordance with the requirements of the Animal Ethics Committee of Bengbu Medical University, the experimental mice were humanely euthanized by cervical dislocation after anesthesia at the end of the study.

2.2 SE Mice Model and Drug Administration

First, anisodamine (1 mg/kg, HY-N0584, MedChemExpress (MCE), Monmouth Junction, NJ, USA) was administered intraperitoneally to mice to reduce peripheral cholinergic effects. After 30 min, pilocarpine (300 mg/kg, P129614, Aladdin, Shanghai, China) was given to induce status epilepticus (SE) [16]. The animals in the control (Ctrl) group were given the same amount of drug solvent.

We first treated the mice with VX765 (HY-13205, MedChemExpress (MCE)) or carbamazepine (CBZ, HY-B0246, MedChemExpress (MCE)) once daily for 4 days via intraperitoneal injection, and then induced the epilepsy model with pilocarpine as described above. The experiment was initially divided into nine groups, nine mice in each group, including a control group (Ctrl group, saline 1 mL/kg), epilepsy groups at 3, 7, 14, and 21 days, VX765 group (200 mg/kg, once a day for 4 days), VX765+SE group, CBZ group (14 mg/kg, once a day for 4 days), and CBZ+SE. The above administrations involved intraperitoneal injection (i.p.). The occurrence and frequency of spontaneous seizures were recorded on video. Mice were intraperitoneally injected with 2% pentobarbital sodium (40 mg/kg, P0225, Tongshan, Shanghai, China) to ensure that the animals were generally anesthetized. After the anesthetic effect was satisfied, the mice were euthanized, and subsequent experiments were conducted.

2.3 Model Evaluation

To determine the effects of VX765 on the intensity of SE, the epileptic seizure grades were evaluated using the Racine Scale. The rating method of epileptic seizures involved the following: Grade I, ear and face convulsions; Grade II, nod; Grade III, anterior limb clonus or posterior limb tilt; Grade IV, bilateral forelimb clonic seizures or standing; and Grade V, repeated tonic clonic seizures or falls. SE was defined as an epileptic seizure lasting more than 5 min. A mouse model with recurrent epileptic seizures for more than 60 min without death was defined as a successful model. If the first administration reached grade IV or above, and the mouse died after the end of administration, it was defined as sudden death, and was eliminated.

2.4 Detection of Inflammatory Factors

An enzyme-linked immunosorbent assay (ELISA) kit (20210326, Jiancheng Bioengineering Institute, Nanjing, Jiangsu, China) was used to analyze the levels of inflammatory cytokines (IL-1β, IL-6, and tumor necrosis factor-alpha [TNF-α]) in the peripheral blood of mice, according to the manufacturer's protocol. Blood was collected from the eyeball and placed in a centrifuge tube. The samples were centrifuged at 3000 rpm for 20 min, the supernatant was preserved and the steps were repeated if there was any sediment. Briefly, inflammatory factors in serum were incubated with the reaction buffer. The sample and biotin antigen were added, and incubated in a 37 °C incubator for 30 min, followed by washing the plate five times in washing solution buffer. Horseradish peroxidase conjugate reagent was then added, and incubated in a 37 °C incubator for 30 min, followed by washing the plate five times. Chromogen solutions A and B were then added and reacted for 10 min at 37 °C. The stop solution was added and the reaction was measured using a microplate reader (Synergy HT, BioTek Instruments, Inc., Winooski, VT, USA). Each sample was analyzed in triplicate. The concentrations of inflammatory cytokines were expressed as ng/L of total protein content. We collected cerebrospinal fluid from 5 non-epileptic con-

trols and 5 patients with epilepsy. The healthy control group used the cerebrospinal fluid from patients who tested negative for treponema pallidum in the cerebrospinal fluid test. The cerebrospinal fluid of patients with epilepsy is the cerebrospinal fluid obtained from patients undergoing lumbar puncture in the neurology department. The cerebrospinal fluid is collected by doctors through lumbar puncture under sterile conditions. Caspase-1 enzyme activity was analyzed using a caspase-1 activity assay kit (C1101, Beyotime, Shanghai, China). Human cerebrospinal fluid (CSF) samples were obtained from 5 patients with epilepsy (mean age 32.6 $\pm$ 8.3 years, 4 males and 1 female) and 5 healthy controls (mean age 35.4 $\pm$ 7.1 years, 3 males and 2 females). Epilepsy patients were diagnosed according to the International League Against Epilepsy (ILAE) criteria and had a mean disease duration of 7.2 $\pm$ 3.5 years. All patients were under stable antiepileptic drug regimens (including levetiracetam, valproate, or carbamazepine). Control CSF samples were obtained from individuals undergoing routine lumbar puncture for suspected non-inflammatory neurological conditions, with normal CSF findings and no history of epilepsy or neuroinflammatory disease.

2.5 Detection of Caspase-1 Activity

Six left hippocampal tissues were homogenized and the protein supernatant was obtained. Caspase-1 enzyme activity in the mouse hippocampal tissue was analyzed using a caspase-1 activity assay kit (C1101, Beyotime). Briefly, the caspase-1-containing tissue supernatant was incubated with the substrate, Ac-YVAD pNA, to generate pNA, and the mixture was incubated at 37 °C for 1–2 h. The activity was then detected at 405 nm using a microplate reader, with each sample analyzed in triplicate.

2.6 Immunohistochemistry

Three whole brains from each group were prepared for immunohistochemical staining. After PBS perfusion, precooled 4% paraformaldehyde (BL539A, Biosharp, Guangzhou, China) was used for perfusion until the mice were stiff. Then, the brain was decapitated, and soaked in 4% paraformaldehyde solution for 24 h, followed by dehydration in 20%–30% sucrose solution for 7 days. After blocking endogenous peroxidase with 3% H_2O_2, serum was added. Then, primary antibody [rabbit antiGFAP (glial fibrillary acidic protein, 1:500, Catalog No. GB11096, Servicebio, Wuhan, Hubei, China), rabbit antiIBA1 (ionized calciumbinding adapter molecule 1, 1:500, Catalog No. GTX635363, GeneTex, Irvine, CA, USA), and mouse antiNeuN (neuronal nuclei, 1:500, Catalog No. ab279296, Abcam, Cambridge, UK)] was added and incubated at 4 °C overnight, followed by washing three times with PBS, every 5 min. The sample was then incubated in secondary antibody (BL003A, Biosharp) for 1 hour at room temperature and washed three times with PBS every 5 min. Then, 3,3 N-diaminobenzidine tetrahydrochloride (DAB, Catalog No. DAB-0031, Biosharp) was added, followed by observation using a microscope, to determine the termination time according to the color. Three slices were randomly taken from each group, and the positive areas and cell numbers of the mouse hippocampus were statistically analyzed using Case Viewer software (2.4.0.119028, Servicebio, Wuhan, Hubei, China).

2.7 Transmission Electron Microscopy

Three right hippocampal tissues were taken after perfusion and transmission electron microscopy analyses. The hippocampal tissues of mice were quickly preserved at 4 °C and the fixative solution and the sampling apparatus were precooled to 4 °C. The hippocampal tissue specimens were cut into small 1-mm pieces and placed in the electron microscope fixation solution (HY-DY3001, MedChemExpress, Monmouth Junction, NJ, USA). After fixation at 4 °C for 2 h, 0.1 M sodium dimethyl arsenate buffer was used for rinsing, three times. Alcohol gradient dehydration was then conducted, with a dehydration time of 10 min for each concentration of alcohol, to a final concentration of 100%. The tissues were then embedded in epoxy resin (14300, Electron Microscopy Sciences, Hatfield, PA, USA) and sectioned. Ultrathin sections were stained with uranyl acetate (22400, Electron Microscopy Sciences) and lead citrate (17800, Electron Microscopy Sciences), and then detected with an H-7500 transmission electron microscope (Hitachi, Tokyo, Japan).

2.8 Western Blotting

Three right hippocampal tissues were used for western blotting. Hippocampal tissue was fully homogenized using a tissue grinder (Cat. No. MagMixA, Magen Biotechnology Co., Ltd., Guangzhou, Guangdong, China) at 60 Hz for a total time of 60 seconds. The sample was then centrifuged at 12,000 rpm for 20 min at 4 °C, followed by the collection of the supernatant. The protein was then denatured at 95 °C for 5 min. The protein samples were then resolved using Sodium Dodecyl Sulfate Polyacrylamide Gel Electrophoresis (SDS-PAGE, E8042, Amresco/Shanghai Jinshan Biotechnology Co., Ltd., Shanghai, China). After electrophoresis, the proteins were transferred to nitrocellulose membranes. A rapid blocking solution (P0252, Beyotime) was used for blocking for 1 hour at room temperature. The membrane was then incubated with the primary antibody at 4 °C overnight. The primary antibodies included rabbit anti-GSDMD (1:1000, G7422, Merck, Sigma-Aldrich, Darmstadt, Germany), mouse anti caspase-1 (AG-20B-0048, AdipoGen Life Sciences, San Diego, CA, USA), B-cell lymphoma 2 (Bcl-2, BL-0062-1, BioSharp), Bcl-2-associated X protein (Bax, BL-0056-1, BioSharp), and mouse anti β-actin (AA128, Beyotime). The membrane was then incubated with secondary antibody for 1 hour at room temperature, then washed with Tween-Phosphate-Buffered Saline (TPBS, ST671, Beyotime) three

times, every 5 min, and then processed using enhanced chemiluminescence reagents (P0018FS, Beyotime). Signals were acquired using a MicroChemi chemiluminescence image analysis system [MicroChemi 4.2 gel documentation system with GelCapture MicroChemi 2.2.0.0 software (DNR Bio-Imaging Systems Ltd., Neve Yamin, Israel)].

2.9 Primary Glial Cells Culture and Construction of Glial Cell-Neuron Models

Fifteen C57BL/6J mice within 72 h of birth were disinfected twice with alcohol, decapitated, and the hippocampus removed. The brain skin and skull were cut along the sagittal suture of the mouse brain, and the pia mater and blood vessels were stripped, leaving the hippocampus. The hippocampus specimens were washed with PBS, then placed in a centrifuge tube, followed by the addition of an appropriate amount of 0.25% trypsin solution (G4004, Servicebio), homogenized with a tissue grinder, mixed with the homogenate, and digested in a 37 °C, 5% CO_2 incubator (51030285, Thermo Fisher Scientific, Waltham, MA, USA) for 15–20 min. Prepared Dulbecco's Modified Eagle Medium/Nutrient Mixture F-12 (DMEM-F12) medium (G4611, Servicebio) was used to terminate the digestion, followed by filtration through a 200-mesh screen, centrifugation at 1000 rpm for 5 min at 4 °C, and then the supernatant discarded. The cell pellet was resuspended with DMEM-F12, inoculated into a tissue culture flask, and placed in an incubator. After 24 h, the DMEM-F12 medium was changed, and then changed every three days.

The purified glial cells were seeded in a large dish or plate for subsequent experiments, 2×10^6cells/well. Lipopolysaccharide (LPS, 100 ng/mL, S1732, Beyotime) was then used to stimulate primary glial cells for 24 h. After removing the supernatant, fresh medium was added and samples were cultured for an additional 24 h. The glial supernatant was taken and added to HT22 hippocampal neuronal cells [17]. The HT22 cell line used in this study was obtained from Rebit Biotechnology Co., Ltd (Shanghai, China) and was cryopreserved at the Scientific Research Center of Bengbu Medical College. The identity of the cell line was verified using short tandem repeat (STR) analysis, which confirmed that the cells were HT22 and free from cross-contamination. Prior to experimentation, the cell line was tested for mycoplasma contamination using polymerase chain reaction (PCR), and the results were negative. For primary glial cells, after 7–10 days of culture, when cells reached 80–90% confluence, the mixed glial population (primarily astrocytes and microglia) was purified by shaking at 200 rpm for 6 h to remove loosely attached microglia. Astrocytes were identified by glial fibrillary acidic protein (GFAP) immunostaining, and microglia by ionized calcium-binding adaptor molecule 1 (IBA1).

2.10 Cell Counting Kit-8 (CCK-8)

The effect of glial supernatant on neuronal function was detected using the CCK-8 cell proliferation assay and flow cytometry. HT22 cells were seeded in 96-well plates at a density of 1×10^4 cells/well.

2.11 Flow Cytometry

Flow cytometry was used to detect the effects of inflammatory glial cell supernatant on neurons, 6 well plates, 2×10^5 cells/well.

2.12 Statistical Analysis

Prism 7.0 software (GraphPad, San Diego, CA, USA) was used to analyze the data. All data are expressed as the mean $\pm$ SEM. One-way or two-way analysis of variance was used for the comparison of multiple groups to determine the statistical significance. Differences were considered to be significant for values of $p < 0.05$.

3. Results

3.1 The Levels of Neuroinflammatory Factors in the Peripheral Serum of SE Mice Were Elevated

Several studies have reported that seizures are accompanied by cerebral neuroinflammation. The epilepsy model was induced with pilocarpine, and spontaneous epileptic seizures occurred on the 0th day, the 3rd day, the 7th day, the 14th day, and the 21st day respectively (Fig. 1A). The results showed that there was no statistically significant difference in seizure number from 0 to 21 days after the epilepsy model was established (Fig. 1B). The severity of the mouse epilepsy model reached its peak on the 21st day (Fig. 1C). To verify whether pilocarpine induced the epileptic mouse model with inflammation, IL-1β and IL-6 in the peripheral serum of mice and the activated caspase-1 in mice brain hippocampus were determined on the 3rd, 7th, 14th, and 21st days in the SE and Ctrl groups after seizures. The results showed that compared with the Ctrl group, the contents of IL-1β, IL-6 and TNF-α in the peripheral serum of the SE group gradually increased, and reached a peak on the 21st day after SE (Fig. 1D,E,F). Compared to the Ctrl group, activated caspase-1 in the hippocampus of the SE group increased with time, and reached a peak on the 21st day (Fig. 1G). These results suggested that the pilocarpine-induced epileptic mouse model was accompanied by significant neuroinflammation. We also collected cerebrospinal fluid from epileptic patients and normal non-epileptic controls to detect the concentrations of IL-1β and IL-6, which were significantly increased. IL-18 and TNF-α showed no statistically significant difference when compared with the normal healthy control group (Fig. 1H). In the pilocarpine-induced mouse model, inflammatory cytokines were assessed in peripheral blood to evaluate systemic immune activation, a well-established surrogate for neuroinflammation in rodent epilepsy studies. In contrast, human inflammatory markers were measured in CSF to directly reflect

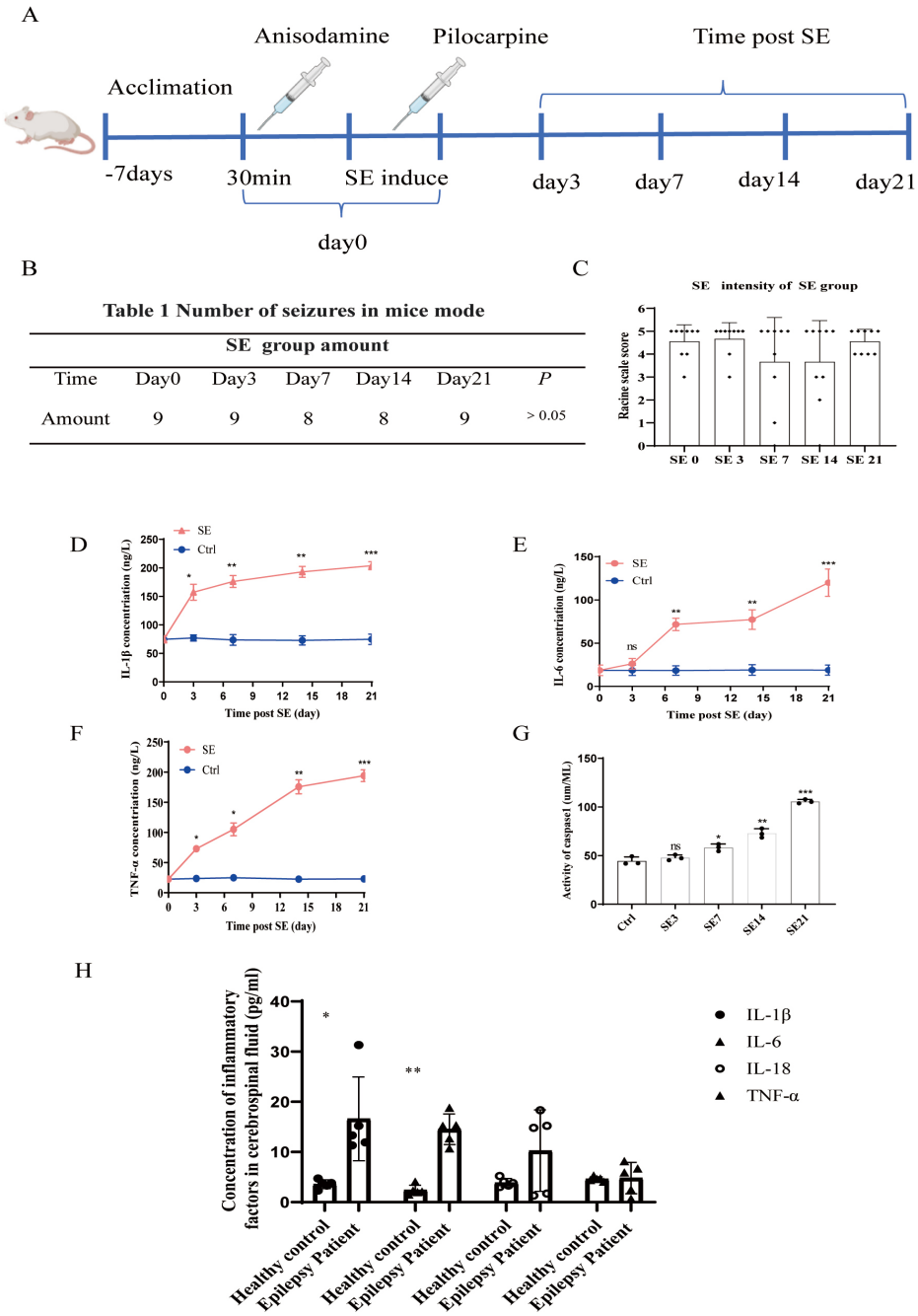

Fig. 1. Pilocarpine-induced neuroinflammation in the peripheral serum of the epileptic mouse model. (A) The pilocarpine-induced epilepsy method on days 3, 7, 14, and 21. (B) Table of seizure numbers of mice in the SE group at different times. (C) Bar graph of seizure intensities of SE mice in the SE group at different times (n = 9/group). (D–F) Contents of inflammatory factors on days 3,7,14, and 21 in the epileptic mouse model. (G) Concentrations of activated caspase-1 on days 3, 7, 14, and 21 in the hippocampal areas of the epileptic mouse model. (H) Histogram of inflammatory factors in the cerebrospinal fluid of healthy and epileptic patients (n = 5/group). ns indicates no statistical significance. *$p < 0.05$; **$p < 0.01$; ***$p < 0.001$. Values are the mean ± SEM. SE, status epilepticus; Ctrl, control; IL, interleukin; TNF-α, tumor necrosis factor-alpha.

central nervous system inflammation, as CSF analysis is clinically routine and more representative of the brain microenvironment in epilepsy patients. Notably, while IL-1β and IL-6 were significantly elevated in patient CSF, IL-18 and TNF-α levels did not differ significantly from controls. This may be due to differences in cytokine dynamics, patient heterogeneity, or the predominant activation of the caspase-1/IL-1β/IL-6 axis in the epileptic inflammatory response.

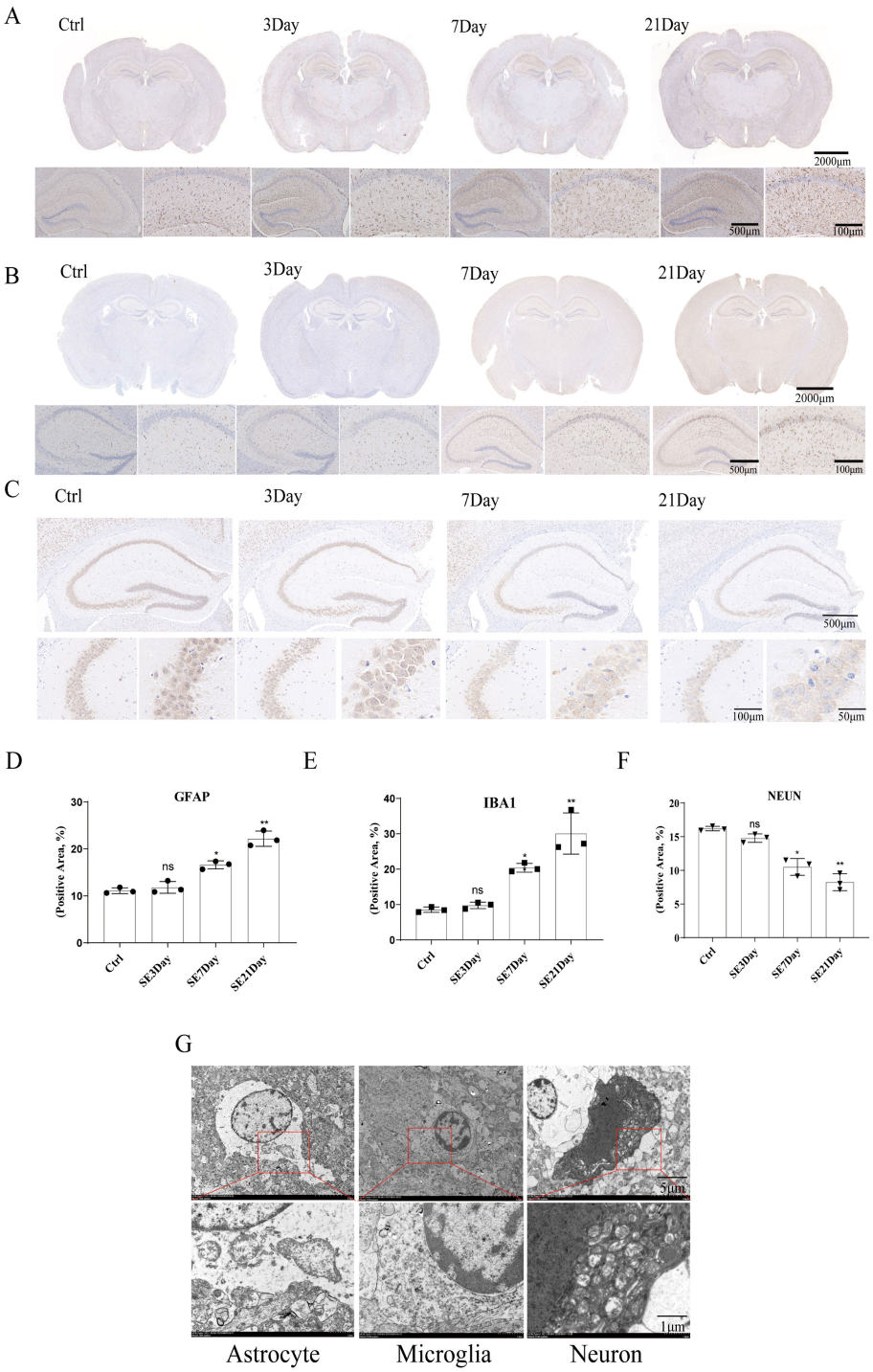

Fig. 2. The activation of astrocytes and microglia, and reduction of neurons in the SE mouse brain induced by pilocarpine. (A,D) Immunohistochemistry. The scale bars are 2000 μm, 500 μm, and 100 μm, respectively. IHC images and bar graphs of the number of activated astrocytes of the SE mouse hippocampus on days 3, 7, and 21 in the control and epilepsy groups. (B,E) IHC images and bar graphs of the number of activated microglia of the SE mouse hippocampus on days 3, 7, and 21 in the control and epilepsy groups. The scale bars are 2000 μm, 500 μm, and 100 μm, respectively. (C,F) IHC images and bar graphs of the reduced numbers of neurons of the mouse hippocampus on days 3, 7, and 21 in the control and epilepsy groups. The scale bars are 500 μm, 100 μm, and 50 μm, respectively. (G) Activation of astrocytes and neuronal apoptosis in the SE mouse brain (n = 3/group). The scale bars are 5 μm and 1 μm. ns indicates not statistically significant. *$p < 0.05$; **$p < 0.01$. GFAP, glial fibrillary acidic protein; IBA1, ionized calcium-binding adaptor molecule 1; NEUN, neuronal nuclei antigen; IHC, immunohistochemistry.

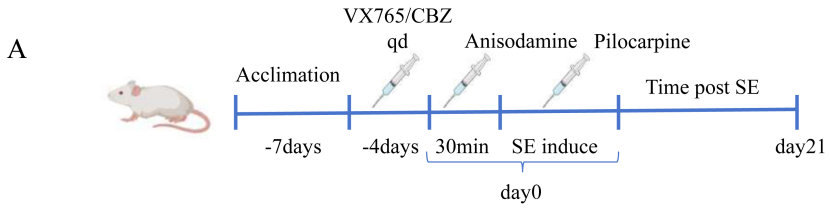

B

Table2 Number of seizures in mice mode

	SE amount						
Group	Ctrl	SE	VX765	VX765+SE	CBZ	CBZ+SE	*P*
Amount	0	9	0	1	0	1	<0.001

C

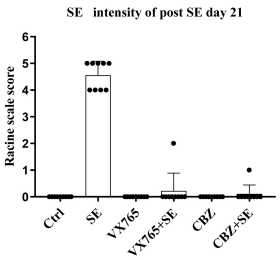

Fig. 3. VX765 suppressed the seizure intensity of the SE mouse. (A) VX765 administration and the pilocarpine-induced epilepsy method. (B) Table of seizure numbers of mice in each group. (C) Bar graph of seizure intensities of SE mice in each group (n = 9/group). CBZ, carbamazepine.

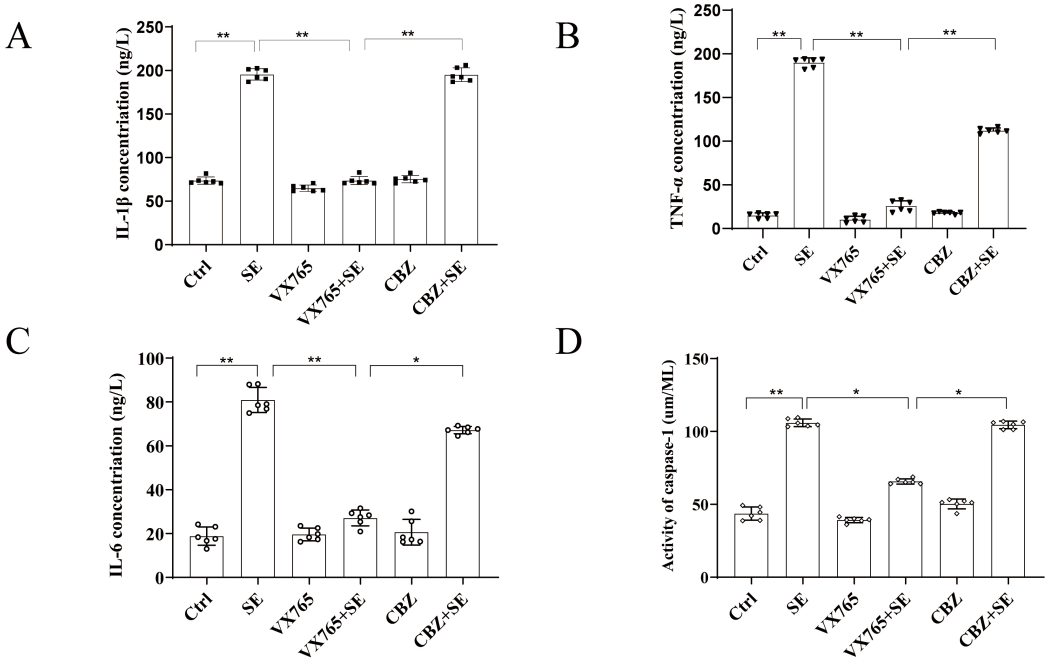

Fig. 4. VX765 reduced neuroinflammation in the hippocampal region of the epileptic mouse model induced by pilocarpine. (A–C) Contents of IL-1β, TNF-α, and IL-6 in the peripheral blood of mice in six groups. (D) Activated caspase-1 in the hippocampus of six groups of mice (n = 6/group). *$p < 0.05$; **$p < 0.01$.

3.2 Hyperactivation of Astrocytes and Microglia, and Apoptosis of Neurons in the Hippocampus of SE Mice

Hippocampal sclerosis, a neuropathological hallmark of temporal lobe epilepsy, is characterized by neuronal loss, gliosis, and synaptic reorganization. Because seizures in epileptic mice were accompanied by a significant increase of inflammatory factors and activated caspase-1 in the hippocampus, we further detected the changes in glial cells and neurons in murine brain tissue. Three mice from each group were selected for immunohistochemistry and electron microscopy assays. The results showed that GFAP-labeled positive cells started to activate during the early stage of SE, and the hyperactivation increased significantly on 7 days after SE, with the largest hyperactivation on the 21st day (Fig. 2A,D). IBA1-labeled positive cells showed no significant activation on day 3, while the activation was significantly increased on days 7 and 21 (Fig. 2B,E). Neuronal nuclei antigen (NEUN)-labeled positive cells continued to

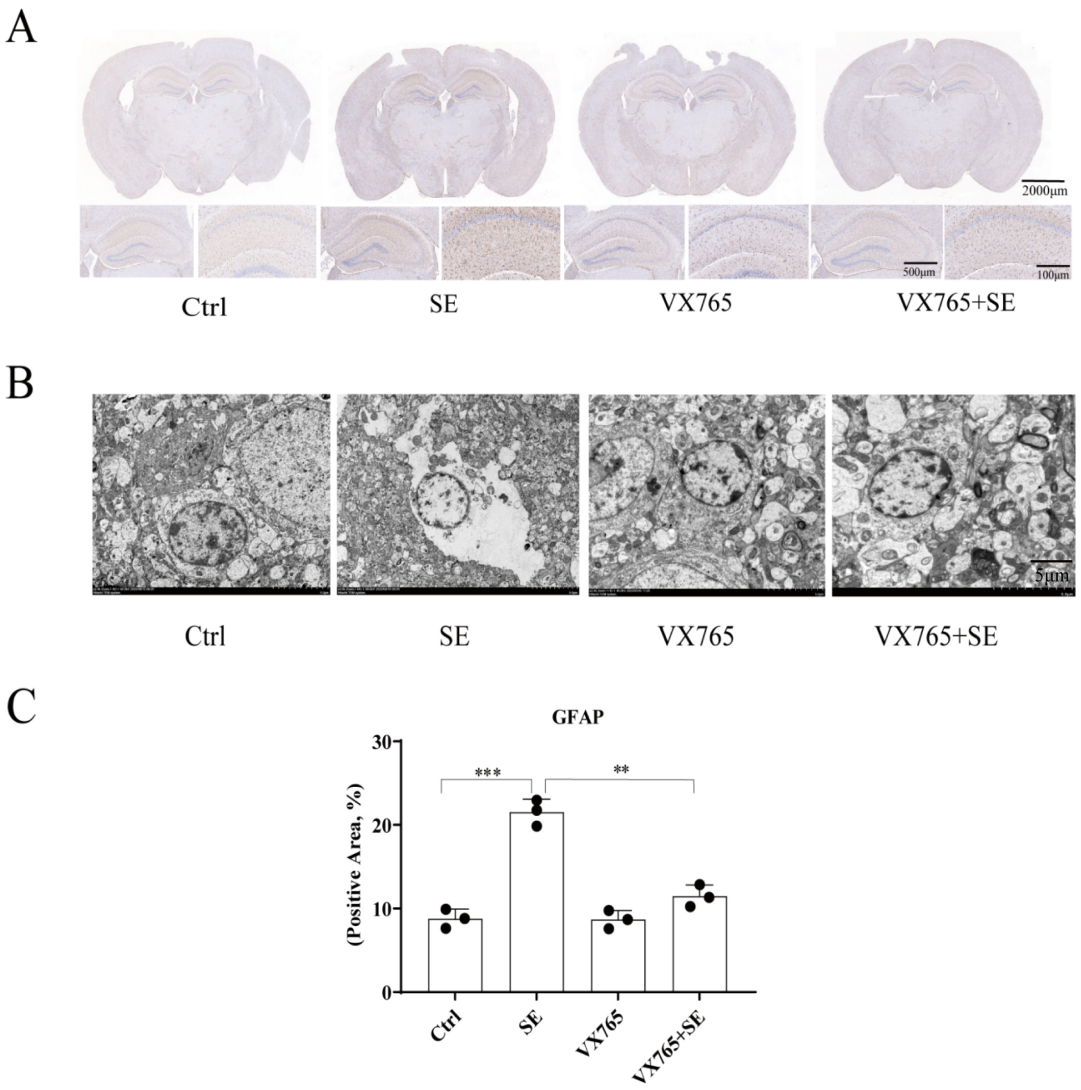

Fig. 5. VX765 reduced activation of astrocytes in the hippocampus of the epileptic mouse model. (A) Immunohistochemistry images of GFAP-stained positive cells. The scale bars are 2000 μm, 500 μm, and 100 μm, respectively. (B) Transmission electron microscopy images of astrocytes. The scale bars are 5 μm. (C) Histogram of the number of GFAP positive cells (n = 3/group). $^{**}p < 0.01$; $^{***}p < 0.001$.

decrease on days 3, 7, and 21 after SE (Fig. 2C,F). The results showed that astrocytes and microglia in the hippocampal region of the brain after SE were swollen and rounded, while the cell membranes were ruptured, with death mainly from pyroptosis. However, death was mainly due to apoptosis, because cell bodies of neurons were atrophic with an intact cell envelope (Fig. 2G). These results showed that seizures were accompanied by hyperactivation of glial cells and apoptosis of neurons.

3.3 VX765 Reduces the Seizure Grade and Number of SE Mice

Epileptic mice were intraperitoneally injected with VX765 or the positive control drug CBZ, both once a day for a total of four times, and then the epilepsy model was induced with pilocarpine (Fig. 3A). The results showed that all nine mice in the SE group had seizures, with seizure levels ranging from 4–5. Both the VX765+SE and CBZ+SE groups had one mouse seizure and seizure levels of grades 2 and 1, respectively (Fig. 3B,C). These results showed that both VX765 and carbamazepine had good anti-epileptic effects, suppressing the intensities of seizures.

3.4 VX765 Reduces Neuroinflammation in the SE Mice

VX765 is a specific inhibitor of caspase-1 and has powerful anti-inflammatory functions under various pathological conditions [18]. ELISA results showed that the levels of IL-1β and IL-6 were significantly increased in the SE group, when compared with the vehicle control group. VX765 treatment significantly inhibited the SE-induced inflammatory cytokine increases of IL-1β, TNF-α and IL-6 (Fig. 4A–C). The caspase-1 results showed that the hip-

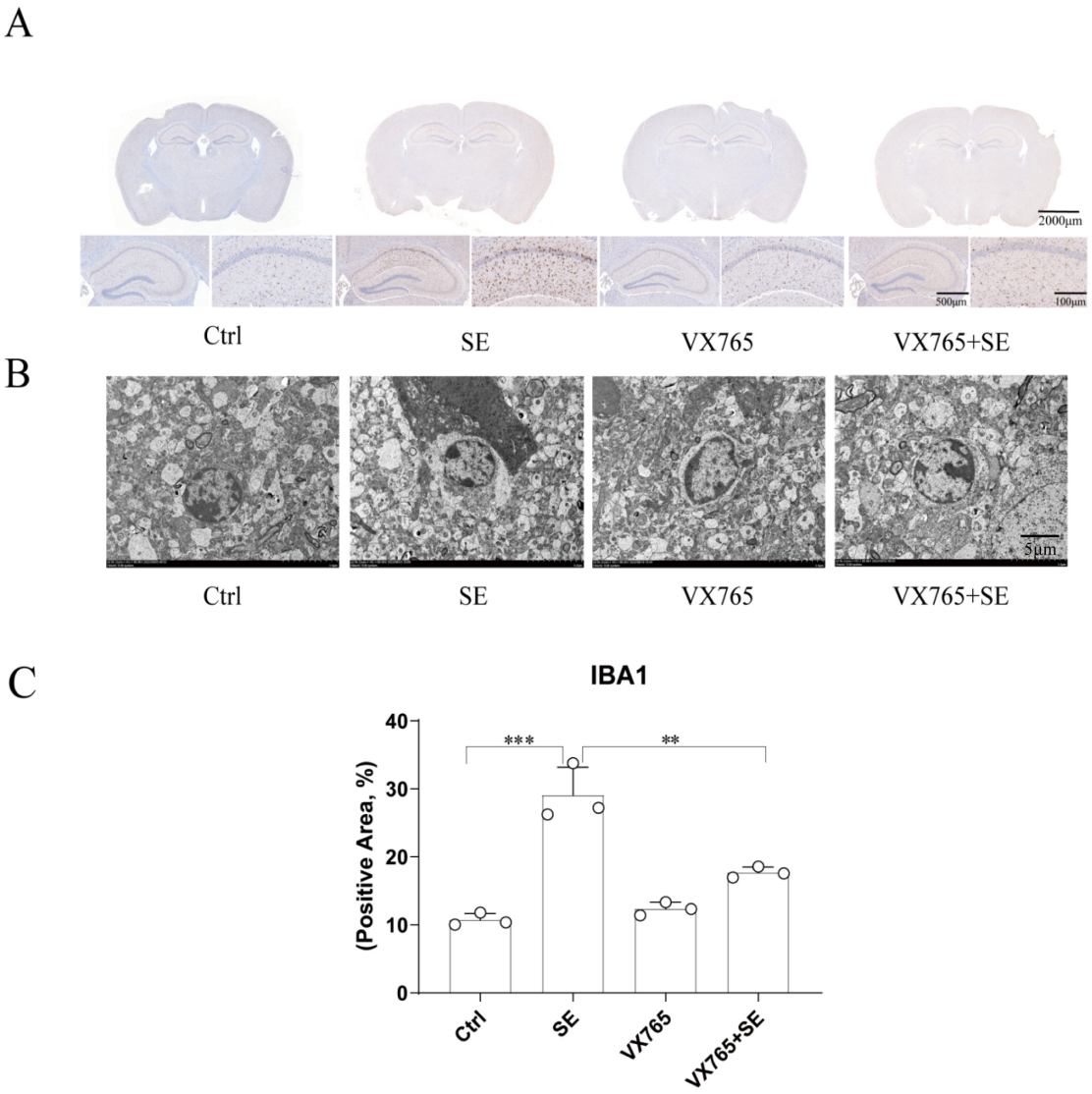

Fig. 6. VX765 reduces the activation of microglia in the hippocampus of the epileptic mouse model. (A) Immunohistochemical image of IBA1-positive cells. The scale bars are 2000 μm, 500 μm, and 100 μm, respectively. (B) Transmission electron microscopy images of microglia. The scale bars are 5 μm. (C) Histogram of IBA1-positive cells (n = 3/group). $^{**}p < 0.01$; $^{***}p < 0.001$.

pocampal caspase-1 activity level significantly increased at day 21 after SE, when compared with the Ctrl group, while VX765 treatment significantly reduced the hippocampal caspase-1 activity induced by SE (Fig. 4D). These results suggested that VX765 inhibited neuroinflammation and peripheral inflammation in the brains and peripheral tissues of epileptic mice induced by pilocarpine.

3.5 VX765 Reduces Hyperactivation of Astrocytes in the Hippocampus of SE Mice

Astrocytes not only play a role in nutritional support for neurons, but also induce neuroinflammation. The immunohistochemistry results showed that the number of GFAP-labeled positive cells in the SE group was significantly higher than in the Ctrl group, and the number of GFAP-labeled positive cells in the VX765+SE group was significantly lower than in the SE group (Fig. 5A,C). The number of astrocytes in the hippocampus of the Ctrl group mice did not significantly increase, and the cell bodies did not swell. Compared with the Ctrl group, the number of astrocytes in the hippocampal region of the SE group was significantly increased, the cells significantly swelled, and cytoplasmic nuclear glycosome depolymerization was observed. Mitochondria, endoplasmic reticulum, and other organelles also showed swelling to varying degrees (Fig. 5B). The VX765 group was similar to the Ctrl group, with the cells having no obvious change. Compared with the SE group, the extent of astrocyte pyroptosis in the VX765+SE group decreased. Together, these results indicated that VX765 inhibited the hyperactivation of astrocytes.

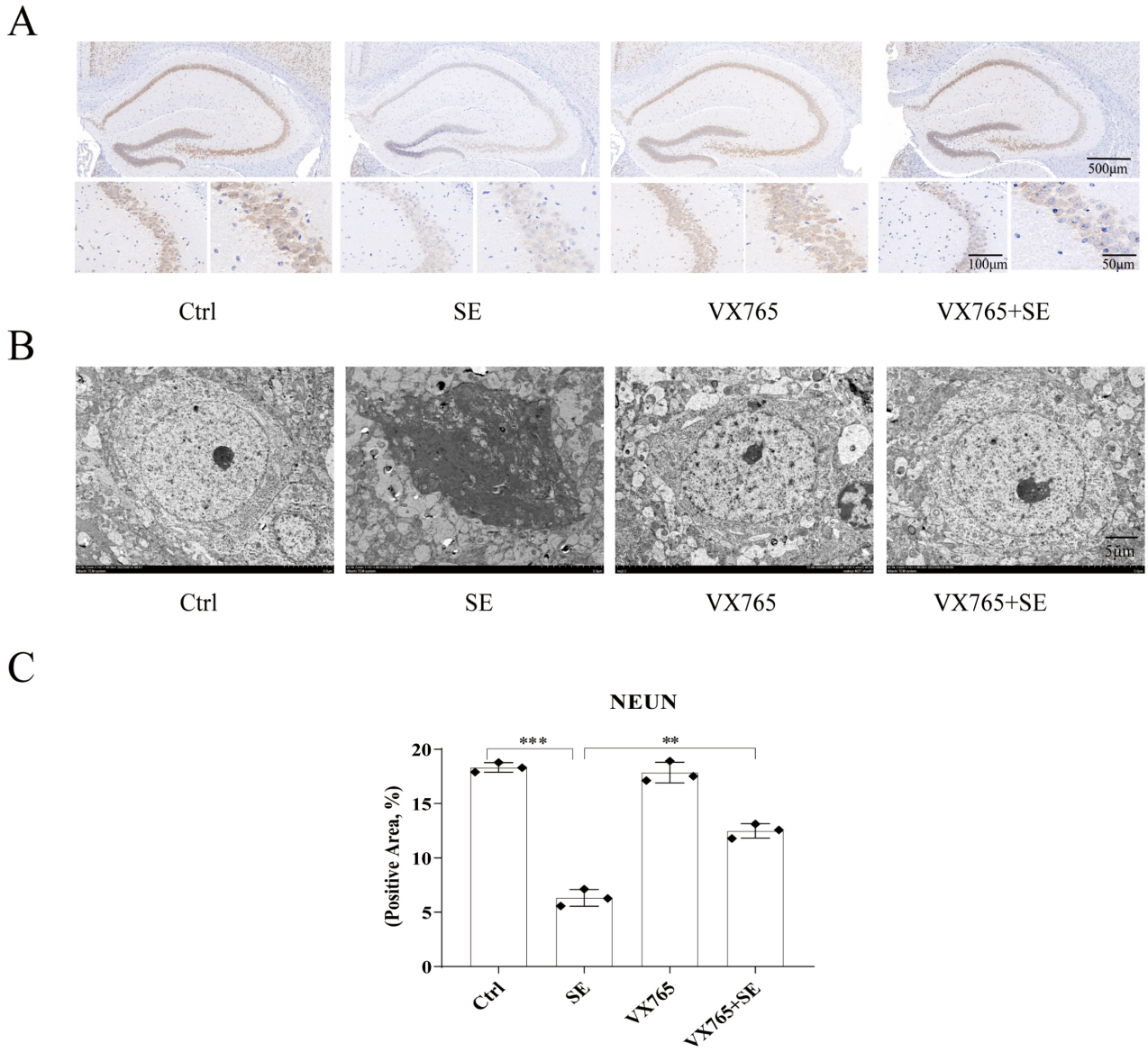

Fig. 7. VX765 reduces damage of neurons in the hippocampus of the epileptic mouse model. (A) Immunohistochemical image of NEUN staining of positive cells. The scale bars are 500 μm, 100 μm, and 50 μm, respectively. (B) Transmission electron microscopy images of neurons. The scale bars are 5 μm. (C) Histogram of NEUN positive cells (n = 3/group). $^{**}p < 0.01$; $^{***}p < 0.001$.

3.6 VX765 Reduces the Hyperactivation of Microglia in the Hippocampus of SE Mice

As the first immune defense line of the nervous system, microglia mediate the secretion of inflammatory factors after proliferation and activation, and play an important role in the development of epilepsy. The results showed that compared with the Ctrl group, the number of IBA1-labeled positive cells was significantly increased in the SE group, but not in the VX765 group. Compared with the SE group, the number of positive IBA1 markers in the VX765+SE group decreased (Fig. 6A,C). The results of electron microscopy showed that compared with the Ctrl group, microglia in the SE group swelled, surrounded the injured neurons, and there were a large number of lipid droplet vacuoles in the activated microglia, which could engulf the damaged apoptotic neurons. Compared with the SE group, the activated microglia in the VX765+SE group were significantly reduced (Fig. 6B). These results indicated that VX765 treatment inhibited the hyperactivation of microglia.

3.7 VX765 Reduces Neuronal Damage in the Hippocampus of SE Mice

Recurrent seizures are accompanied by abnormal firing and reduction of neurons. The results showed that compared with the Ctrl group, neuronal cells in the hippocampus of the SE group were significantly lost, while there was no significant change in the VX765 group, when compared

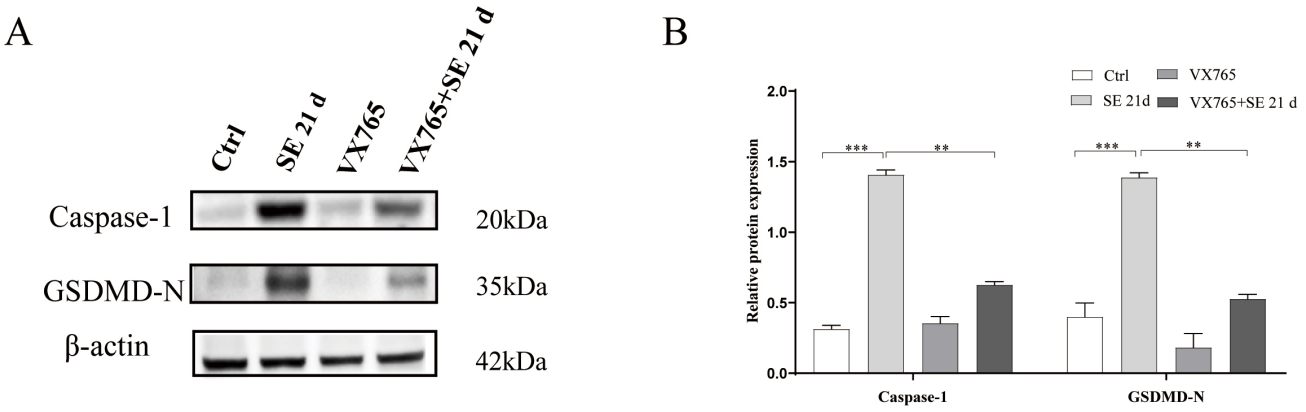

Fig. 8. VX765 reduces the expressions of caspase-1 and GSDMD-N, in the hippocampus of the epileptic mouse model. (A) Expression bands (western blotting) of caspase-1 and GSDMD-N proteins in the hippocampus. (B) Histogram of caspase-1 and GSDMD-N protein expressions. $^{**}p < 0.01$; $^{***}p < 0.001$. GSDMD-N, Gasdermin D N-terminal; d,day.

with the Ctrl group. Compared with the SE group, the neuron loss in the VX765+SE group was significantly reduced (Fig. 7A,C). The results of electron microscopy showed that compared with the Ctrl group, neurons in SE group were pyknotic, the electron densities of cytoplasm and processes increased, and the chromatin in the nucleus was highly condensed, indicating that neuronal cells underwent apoptosis. There was no significant change in neurons in the VX765 group. The apoptosis of neurons in the VX765+SE group was significantly lower than that in the SE group (Fig. 7B). Together, these results indicated that VX765 had a neuroprotective effect.

3.8 VX765 Reduces the Expressions of Caspase-1 and GSDMD-N in the Hippocampus of SE Mice

To determine the effect of VX765 on glial hyperactivation, the supernatant of the hippocampal tissue homogenate was used to extract proteins, and the expressions of caspase-1 and Gasdermin D N-terminal (GSDMD-N)were detected. The results showed that compared with the Ctrl group, the expressions of caspase-1 and GSDMD-N were significantly increased in the SE group, while there was no significant change in the VX765 group, when compared with the Ctrl group. The expressions of caspase-1 and GSDMD-N in the VX765+SE group were significantly lower than those in the SE group (Fig. 8A,B; The original western blotting images can be found in the **Supplementary Materials**). These results further indicate that VX765 can alleviate the excessive activation of nerve cells in the hippocampal region of the SE mice.

3.9 VX765 Reduces Apoptosis of HT22 Neurons Induced by the Glial Inflammatory Supernatant

To further characterize its mechanism, we conducted cell experiments involving cultured primary glia and hippocampal neuronal cells (HT22), and verified that VX765 exerted neuronal protection by inhibiting glial hyperactivation. The glia-neuron co-culture model was prepared according to Fig. 9A. Compared to the Ctrl group, the apoptosis of HT22 cells in the glial conditioned medium (CMG) group increased significantly, and the apoptosis of HT22 in the VX765+CMG group was significantly decreased compared with the CMG group (Fig. 9B,C). The CCK-8 results showed that when HT22 was stimulated with LPS, no neuronal death occurred, and there was no statistical difference among the four groups. When HT22 was stimulated with the CMG, compared with the Ctrl group, the survival of HT22 in the CMG group was significantly reduced, and the survival of HT22 in the CMG+VX765 group was significantly improved, when compared with that of the CMG group (Fig. 9D,E). Western blotting results showed that when compared with the Ctrl group, Bax expression in the CMG group increased significantly, whereas Bcl-2 expression decreased (Fig. 9F,G; The original western blotting images can be found in the **Supplementary Materials**). Together, the results showed that LPS induced glial cells to secrete an inflammatory factor rich supernatant, which may have induced neuronal apoptosis. VX765 may have protected neurons by regulating glial hyperactivation, reducing the secretion of inflammatory factors, and inhibiting neuronal apoptosis (Fig. 10).

4. Discussion

The main mechanisms by which glial cells promote the development of seizures and epilepsy include increased excitability and inflammation. Uncontrolled glial-mediated immune responses can cause sustained inflammatory changes and promote epileptogenesis [19]. The inflammatory state after astrocyte changes may be the main cause of mesial temporal lobe epilepsy with sclerosis, which is usually described as upregulation of GFAP [20]. Astrocytes in spontaneously epileptic mice became activated, accompanied by increased expression of glial fibrillary acidic protein [21]. This is also consistent with our results, hyperactivation of the number of microglia and astrocytes increased

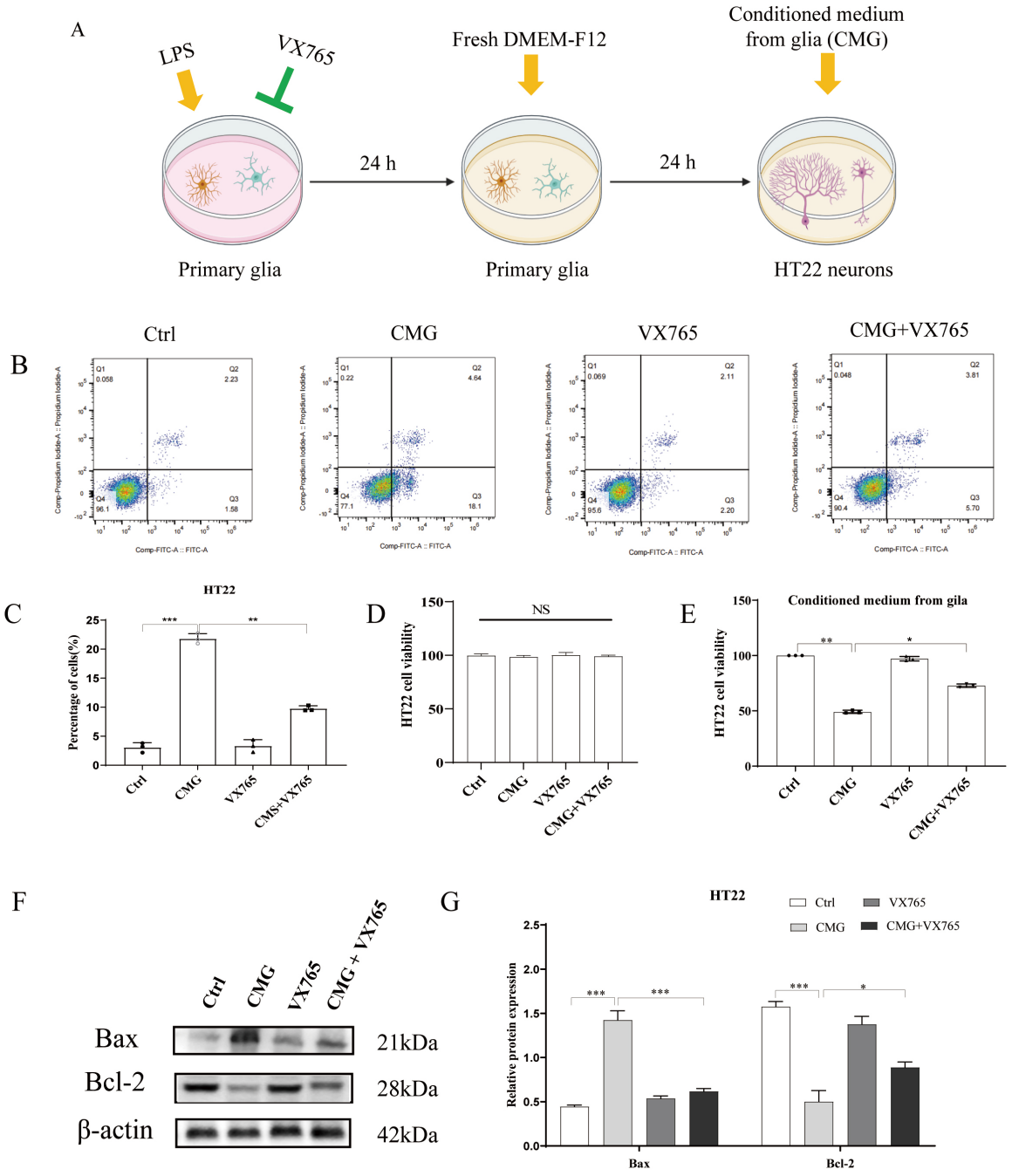

Fig. 9. VX765 improves the survival of HT22 cells. (A) Methodology of the cell experimental model. The yellow arrows indicate the addition of the above mentioned drugs or culture medium to the culture dish, while the green arrow represents the addition of VX765 to the culture dish to inhibit caspase-1, thereby suppressing the secretion of inflammatory factors. (B) Flow cytometry results of apoptosis of HT22 cells. (C) Histogram of the apoptosis of HT22 cells. (D,E) CCK-8 cell proliferation assay results of HT22 cells. NS means Normal Saline (0.9% NaCl). (F) Expressions of the apoptosis-related proteins. (G) Quantification plot of the protein results. *$p < 0.05$; **$p < 0.01$; ***$p < 0.001$. LPS, lipopolysaccharide; DMEM-F12, Dulbecco's Modified Eagle Medium/Nutrient Mixture F-12; CMG, glial conditioned medium; CCK-8, cell counting kit-8.

significantly and showed pyroptosis features such as organelle swelling, while the number of neurons decreased significantly and showed cytological features of apoptosis. Dimethyl fumarate significantly reduced inflammatory factors such as IL-18 and IL-1β, and the number of astrocytes and microglia on days 7–21 after epilepsy [22]. In both human chronic epilepsy and animal experiments, IL-1β is significantly elevated. In epileptogenic brain tissue, both microglia and astrocytes are sources of IL-1β, while IL-1 type receptors (IL-1R1) mediate IL-1β biological effects, which

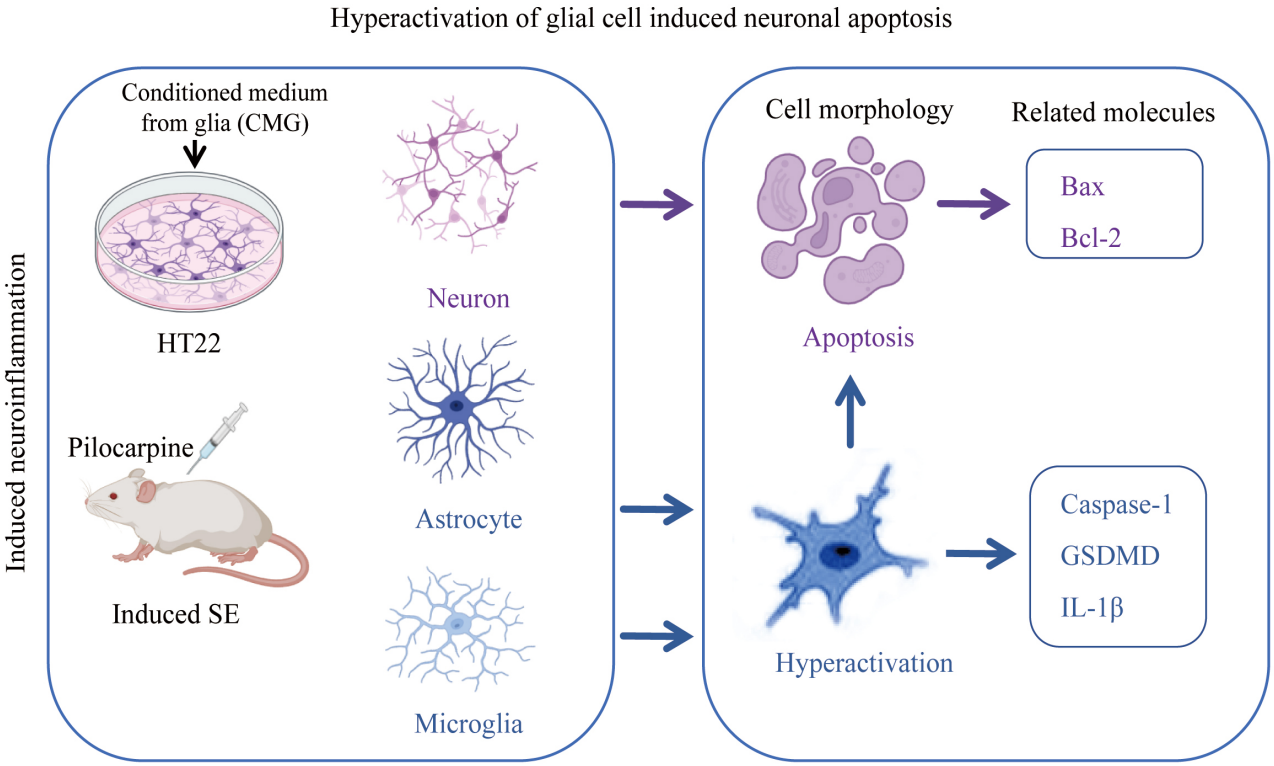

Fig. 10. Pilocarpine induced the frequency of epilepsy in mice, promoted the excessive release of glial inflammatory factors, and resulted in neuronal apoptosis. The blue arrows indicate the effects of glial cells, and the purple arrows indicate the effects of neurons. Bax, Bcl-2-associated X protein; Bcl-2, B-cell lymphoma 2.

are overexpressed in both neurons and glia [23,24]. In the present study, we showed that neuroinflammatory factors were significantly increased in an epileptic mouse model, and reached a peak on the 21st day after SE. In addition, activated caspase-1 in the hippocampus of the SE group increased with time and reached a peak on the 21st day.

By inhibiting neuroinflammation, increasing evidence shows that VX765 is beneficial to a variety of neurological diseases. VX765 attenuated the High Mobility Group Box 1/Toll-like Receptor 4/Nuclear Factor Kappa B (HMGB1/TLR4/NF-κB) signaling pathway to inhibit the inflammatory response of the murine TBI model, to promote nerve recovery [25]. VX765 had a protective effect on endothelial cell pyroptosis and barrier dysfunction induced by lung ischemia/reperfusion [26]. VX765 reduced Intestinal Ischemia-Reperfusion Injury (IIRI)-induced oxidative stress and inflammatory response *in vivo* and *in vitro*, while reducing the levels of IL-1β and IL-6 [27]. VX765 reversed astrocyte pyroptosis and improved behavioral deterioration in astrocyte Kir6.1 knockout mice [28]. In the present study, VX765 can significantly alleviate the frequency and intensity of seizures in epileptic mice, and reduce the levels of proinflammatory factors in peripheral blood and caspase1 enzyme activity in hippocampus, as well as the hyperactivation of glial cells and neuronal apoptosis.

Glial cells are closely related to a variety of neuronal functions, such as, activated microglia promote the hyperactivation of astrocytes. However, when microglia are overactivated, they will release excessive inflammatory factors, causing neurotoxicity [29]. Activated microglia will secrete IL-1, and the released IL-1 will further stimulate hyperactivation of microglia, eventually leading to neuronal damage. IL-1β can be detected in microglia after seizures, but its expression disappears after a few hours. Nevertheless, microglia are still activated, as if they are in a primed state [30]. Cannabidiol inhibited the hyperactivation of microglia and alleviated neuronal damage caused by kainic acid [31]. Purinergic receptor P2X7 (P2X7R) was involved in promoting depression and anxiety-like behavior in pilocarpine-induced epileptic rats. The P2X7R antagonist was used to produce direct antidepressant and anxiolytic effects. P2X7R antagonist did not affect the development of spontaneous seizure recurrence, and it played a protective role in nerves by inhibiting the hyperactivation of microglia after SE [32]. IL-10 inhibited IL-1β during seizures involving the production and hyperactivation of inflammatory microglia [33]. In our study, *in vitro* experiments showed that CMG promoted apoptosis of HT22 neurons through Bax and Bcl-2, and VX765 could alleviate the apoptosis of HT22 neurons by inhibiting the secretion of inflammatory factors by glial cells.

5. Conclusions

The pilocarpine-induced epilepsy model exhibited increased inflammatory factors and glial hyperactivation. VX765 treatment reduced glial hyperactivation and neuronal loss, attenuating epileptic progression. Its neuroprotective mechanism may involve inhibiting glial inflammatory factor release and reducing neuronal apoptosis. *In vivo*, VX765 concurrently suppressed glial activation and neuronal apoptosis. *In vitro*, VX765 alleviated neuronal apoptosis induced by glial inflammatory factors, suggesting that its neuroprotective effects may be mediated through the regulation of glial activation and inflammatory responses. It should be noted that the *in vitro* model cannot fully replicate the *in vivo* microenvironment, providing only preliminary insights. In this study, VX765 was administered prophylactically, which differs from clinical practice where treatment begins after unpredictable seizures. Future studies should evaluate its efficacy when given after epilepsy establishment to better assess translational relevance. Future studies using advanced techniques like co-culture systems or live imaging could further elucidate the temporal and causal relationships between glial activation and neuronal injury in epilepsy.

Availability of Data and Materials

The data that support the findings of this study are available from the corresponding author upon reasonable request.

Author Contributions

HC finished the animal study and was responsible for the *in vitro* study, wrote the manuscript. XZ finished the animal study, were responsible for the *in vitro* study. XX analyzed data and constructed the graphs. ZL analyzed data and revised the manuscript. HL designed the study. YS designed the study, analyzed data and constructed the graphs, revised the manuscript. All authors contributed to editorial changes in the manuscript. All authors read and approved the final manuscript. All authors have participated sufficiently in the work and agreed to be accountable for all aspects of the work.

Ethics Approval and Consent to Participate

All animal experimental protocols were reviewed and approved by the Institutional Animal Care and Use Committee of Bengbu Medical University (Approval No. 2021-105). The animal experiments described in this study were conducted in strict accordance with the ARRIVE guidelines and the National Institutes of Health (NIH) Guide for the Care and Use of Laboratory Animals (8th edition, 2011).

Written informed consent was obtained from all participants before their involvement in this study. The consent process was conducted in accordance with the ethical standards of the Declaration of Helsinki and was reviewed and approved by the Medical Research Ethics Committee of Bengbu Medical University (Approval No. 440 of 2025). The consent forms clearly explained the purpose, procedures, potential risks, and benefits of the study, and participants were informed of their right to withdraw at any time without penalty.

Acknowledgment

Not applicable.

Funding

This work was supported by the Natural Science Foundation of China (82104152), Cultivation program for middle and young teachers in universities (YQYB2025016).

Conflicts of Interest

The authors declare no conflicts of interest.

Supplementary Material

Supplementary material associated with this article can be found, in the online version, at https://doi.org/10.31083/JIN49777.

References

[1] Devinsky O, Vezzani A, O'Brien TJ, Jette N, Scheffer IE, de Curtis M, *et al*. Epilepsy. Nature Reviews. Disease Primers. 2018; 4: 18024. https://doi.org/10.1038/nrdp.2018.24.

[2] Steriade C, Titulaer MJ, Vezzani A, Sander JW, Thijs RD. The association between systemic autoimmune disorders and epilepsy and its clinical implications. Brain. 2021; 144: 372–390. https://doi.org/10.1093/brain/awaa362.

[3] Huberfeld G, Blauwblomme T, Miles R. Hippocampus and epilepsy: Findings from human tissues. Revue Neurologique. 2015; 171: 236–251. https://doi.org/10.1016/j.neurol.2015.01.563.

[4] Kamali AN, Zian Z, Bautista JM, Hamedifar H, Hosseinkhannazer N, Hosseinzadeh R, *et al*. The Potential Role of Pro-Inflammatory and Anti-Inflammatory Cytokines in Epilepsy Pathogenesis. Endocrine, Metabolic & Immune Disorders Drug Targets. 2021; 21: 1760–1774. https://doi.org/10.2174/1871530320999201116200940.

[5] Sanz P, Garcia-Gimeno MA. Reactive Glia Inflammatory Signaling Pathways and Epilepsy. International Journal of Molecular Sciences. 2020; 21: 4096. https://doi.org/10.3390/ijms21114096.

[6] von Bernhardi R, Eugenín-von Bernhardi J, Flores B, Eugenín León J. Glial Cells and Integrity of the Nervous System. Advances in Experimental Medicine and Biology. 2016; 949: 1–24. https://doi.org/10.1007/978-3-319-40764-7_1.

[7] Eyo UB, Murugan M, Wu LJ. Microglia-Neuron Communication in Epilepsy. Glia. 2017; 65: 5–18. https://doi.org/10.1002/glia.23006.

[8] Purnell BS, Alves M, Boison D. Astrocyte-neuron circuits in epilepsy. Neurobiology of Disease. 2023; 179: 106058. https://doi.org/10.1016/j.nbd.2023.106058.

[9] Devinsky O, Vezzani A, Najjar S, De Lanerolle NC, Rogawski MA. Glia and epilepsy: excitability and inflammation. Trends in Neurosciences. 2013; 36: 174–184. https://doi.org/10.1016/j.tins.2012.11.008.

[10] Kaczorowska M, Czekuć-Kryśkiewicz E, Dądalski M, Kotulska

K. Immunological markers of drug resistant epilepsy and its response to immunomodulatory therapy with ACTH in children. Folia Neuropathologica. 2023; 61: 360–370. https://doi.org/10.5114/fn.2023.131662.

[11] Jiang Q, Tang G, Zhong XM, Ding DR, Wang H, Li JN. Role of Stat3 in NLRP3/caspase-1-mediated hippocampal neuronal pyroptosis in epileptic mice. Synapse. 2021; 75: e22221. https://doi.org/10.1002/syn.22221.

[12] Atabaki R, Khaleghzadeh-Ahangar H, Esmaeili N, Mohseni-Moghaddam P. Role of Pyroptosis, a Pro-inflammatory Programmed Cell Death, in Epilepsy. Cellular and Molecular Neurobiology. 2023; 43: 1049–1059. https://doi.org/10.1007/s10571-022-01250-3.

[13] Evavold CL, Ruan J, Tan Y, Xia S, Wu H, Kagan JC. The Pore-Forming Protein Gasdermin D Regulates Interleukin-1 Secretion from Living Macrophages. Immunity. 2018; 48: 35–44.e6. https://doi.org/10.1016/j.immuni.2017.11.013.

[14] Gonzalez-Giraldo E, Sullivan JE. Advances in the Treatment of Drug-Resistant Pediatric Epilepsy. Seminars in Neurology. 2020; 40: 257–262. https://doi.org/10.1055/s-0040-1702941.

[15] Xu XE, Liu L, Wang YC, Wang CT, Zheng Q, Liu QX, *et al*. Caspase-1 inhibitor exerts brain-protective effects against sepsis-associated encephalopathy and cognitive impairments in a mouse model of sepsis. Brain, Behavior, and Immunity. 2019; 80: 859–870. https://doi.org/10.1016/j.bbi.2019.05.038.

[16] Vizuete AFK, Hansen F, Negri E, Leite MC, de Oliveira DL, Gonçalves CA. Effects of dexamethasone on the Li-pilocarpine model of epilepsy: protection against hippocampal inflammation and astrogliosis. Journal of Neuroinflammation. 2018; 15: 68. https://doi.org/10.1186/s12974-018-1109-5.

[17] Li Y, Li J, Yang L, Ren F, Dong K, Zhao Z, *et al*. Ginsenoside Rb1 protects hippocampal neurons in depressed rats based on mitophagy-regulated astrocytic pyroptosis. Phytomedicine. 2023; 121: 155083. https://doi.org/10.1016/j.phymed.2023.155083.

[18] Wang YH, Tang YR, Gao X, Liu J, Zhang NN, Liang ZJ, *et al*. The anti-inflammatory and analgesic effects of intraperitoneal melatonin after spinal nerve ligation are mediated by inhibition of the NF-κB/NLRP3 inflammasome signaling pathway. Brain Research Bulletin. 2021; 169: 156–166. https://doi.org/10.1016/j.brainresbull.2021.01.015.

[19] Zhu X, Yao Y, Yang J, Ge Q, Niu D, Liu X, *et al*. Seizure-induced neuroinflammation contributes to ectopic neurogenesis and aggressive behavior in pilocarpine-induced status epilepticus mice. Neuropharmacology. 2020; 170: 108044. https://doi.org/10.1016/j.neuropharm.2020.108044.

[20] Boison D, Steinhäuser C. Epilepsy and astrocyte energy metabolism. Glia. 2018; 66: 1235–1243. https://doi.org/10.1002/glia.23247.

[21] Thompson JA, Miralles RM, Wengert ER, Wagley PK, Yu W, Wenker IC, *et al*. Astrocyte reactivity in a mouse model of SCN8A epileptic encephalopathy. Epilepsia Open. 2022; 7: 280–292. https://doi.org/10.1002/epi4.12564.

[22] Xia L, Liu L, Cai Y, Zhang Y, Tong F, Wang Q, *et al*. Inhibition of Gasdermin D-Mediated Pyroptosis Attenuates the Severity of Seizures and Astroglial Damage in Kainic Acid-Induced Epileptic Mice. Frontiers in Pharmacology. 2022; 12: 751644. https://doi.org/10.3389/fphar.2021.751644.

[23] Boer K, Jansen F, Nellist M, Redeker S, van den Ouweland AMW, Spliet WGM, *et al*. Inflammatory processes in cortical tubers and subependymal giant cell tumors of tuberous sclerosis complex. Epilepsy Research. 2008; 78: 7–21. https://doi.org/10.1016/j.eplepsyres.2007.10.002.

[24] Ravizza T, Noé F, Zardoni D, Vaghi V, Sifringer M, Vezzani A. Interleukin Converting Enzyme inhibition impairs kindling epileptogenesis in rats by blocking astrocytic IL-1beta production. Neurobiology of Disease. 2008; 31: 327–333. https://doi.org/10.1016/j.nbd.2008.05.007.

[25] Sun Z, Nyanzu M, Yang S, Zhu X, Wang K, Ru J, *et al*. VX765 Attenuates Pyroptosis and HMGB1/TLR4/NF-κB Pathways to Improve Functional Outcomes in TBI Mice. Oxidative Medicine and Cellular Longevity. 2020; 2020: 7879629. https://doi.org/10.1155/2020/7879629.

[26] Wu S, Li Z, Ye M, Liu C, Liu H, He X, *et al*. VX765, a Specific Caspase-1 Inhibitor, Alleviates Lung Ischemia Reperfusion Injury by Suppressing Endothelial Pyroptosis and Barrier Dysfunction. BioMed Research International. 2021; 2021: 4525988. https://doi.org/10.1155/2021/4525988.

[27] Lyu H, Ni H, Huang J, Yu G, Zhang Z, Zhang Q. VX-765 prevents intestinal ischemia-reperfusion injury by inhibiting NLRP3 inflammasome. Tissue & Cell. 2022; 75: 101718. https://doi.org/10.1016/j.tice.2021.101718.

[28] Li F, Jiang SY, Tian T, Li WJ, Xue Y, Du RH, *et al*. Kir6.1/K-ATP channel in astrocytes is an essential negative modulator of astrocytic pyroptosis in mouse model of depression. Theranostics. 2022; 12: 6611–6625. https://doi.org/10.7150/thno.77455.

[29] Liu W, Tang Y, Feng J. Cross talk between activation of microglia and astrocytes in pathological conditions in the central nervous system. Life Sciences. 2011; 89: 141–146. https://doi.org/10.1016/j.lfs.2011.05.011.

[30] Ravizza T, Gagliardi B, Noé F, Boer K, Aronica E, Vezzani A. Innate and adaptive immunity during epileptogenesis and spontaneous seizures: evidence from experimental models and human temporal lobe epilepsy. Neurobiology of Disease. 2008; 29: 142–160. https://doi.org/10.1016/j.nbd.2007.08.012.

[31] Landucci E, Mazzantini C, Lana D, Calvani M, Magni G, Giovannini MG, *et al*. Cannabidiol inhibits microglia activation and mitigates neuronal damage induced by kainate in an in-vitro seizure model. Neurobiology of Disease. 2022; 174: 105895. https://doi.org/10.1016/j.nbd.2022.105895.

[32] Hong S, Xin Y, JiaWen W, ShuQin Z, GuiLian Z, HaiQin W, *et al*. The P2X7 receptor in activated microglia promotes depression- and anxiety-like behaviors in lithium -pilocarpine induced epileptic rats. Neurochemistry International. 2020; 138: 104773. https://doi.org/10.1016/j.neuint.2020.104773.

[33] Sun Y, Ma J, Li D, Li P, Zhou X, Li Y, *et al*. Interleukin-10 inhibits interleukin-1β production and inflammasome activation of microglia in epileptic seizures. Journal of Neuroinflammation. 2019; 16: 66. https://doi.org/10.1186/s12974-019-1452-1.